Astron. Astrophys. 335, 979–984 (1998)

ASTRONOMY AND ASTROPHYSICS

Polarimetry and spectroscopy of the polar RX J1141.3-6410⋆

C.V. Rodrigues[1,2], **D. Cieslinski**[2,1], **and J.E. Steiner**[2,3]

[1] Div. Astrofísica, Instituto Nacional de Pesquisas Espaciais/MCT, Caixa Postal 515, 12201-970, São José dos Campos, SP, Brazil
[2] Departamento de Astronomia, Instituto Astronômico e Geofísico/USP, Caixa Postal 9638, 01065-970 São Paulo, SP, Brazil
[3] Laboratório Nacional de Astrofísica/CNPq/MCT, Av. Estados Unidos, 154, 37500-000 Itajubá, MG, Brazil

Received 12 September 1997 / Accepted 21 April 1998

Abstract. We present the first optical polarimetric measurements of RX J1141.3-6410 which confirm that star as a polar. The circular polarization varies between 0 and 13% with the orbital period. Hα spectroscopy shows that this line is formed by, at least, two components: a broad and a narrow one. The phase of maximum redshift of the broad component is shifted by 0.5 with the phase of maximum circular polarization which is not usual for this class of stars. We suggest a geometrical configuration for the system which could explain the main features of the polarimetric and spectroscopic data.

Key words: stars: individual: RX J1141.3-6410 – stars: novae, cataclysmic variables – stars: magnetic fields – accretion, accretion disks – polarization – X-rays: stars

1. Introduction

Cataclysmic variables (CVs) are binaries consisting of a red main sequence star and a white dwarf (primary). The secondary fills its Roche lobe and mass is transfered to the white dwarf (WD). This process usually forms an accretion disk. However, some CVs have a magnetic field intense enough to prevent the disk formation. In this case, the matter falls onto the WD near the magnetic pole forming an accretion column. Another important consequence of the high strength of the magnetic field is the synchronization of the white dwarf rotation with the orbital movement. These stars are denominated polars and their prototype is AM Her. Reviews can be found in Cropper (1990) and Warner (1995). The polars can be distinguished from intermediate polars (non-synchronized magnetic systems) by two important features: high circular polarization and strong soft X-ray emission. The former is caused by cyclotron emission in the column. The emission at high frequencies is produced by the shock formed close to the WD surface.

The emission lines in polars are thought to be formed along the trajectory of the material from the secondary to the white dwarf (see review by Mukai 1988). This material leaves the secondary at the inner Lagrangian point (L_1) and follows its ballistic trajectory in the orbital plane (horizontal stream) down to the coupling region. In this region the magnetic pressure becomes higher than the ram pressure and the material starts to follow the magnetic lines (accretion stream). The radiation produced near the white dwarf can be reprocessed on the secondary surface contributing to the emission lines.

The emission lines of polars can be formed by up to four components (Rosen et al. 1987, e.g.). In general, at least two components are seen: a broad base component and a narrow peak component. The accretion stream is responsible for the broad component. The narrow one is formed nearer the secondary. In some systems, this emission seems to be formed on the secondary surface itself (Liebert & Stockman 1985). In others, there is evidence that the horizontal stream produces such emission (Mukai 1988).

Recently, Doppler tomography of polars has improved the understanding of the emission lines (Diaz & Steiner 1994; Schwope et al. 1997; Šimić et al. 1998). An important fraction of the emission seems to be produced near the secondary. The bulk of the broad component is formed near the coupling region. These maps do not show an important emission from the region of high velocities near the white dwarf.

Many sources identified by the ROSAT satellite have been shown to be CVs and, more specifically, polars. Motch et al. (1996) discovered 7 new CVs and suggested that two of them could be synchronized magnetic systems based on the strength of their emission lines. RX J1141.3-6410 is one of these systems. It is associated with a ≈16.5 mag star having a strong He II λ4686 emission line. Recently, Cieslinski & Steiner (1997) have found a photometric period (P = 0.131 517 d) and a light curve consistent with the suggestion of RX J1141.3-6410 being a polar. However, until now, no polarimetric measurement has been made in order to confirm its magnetic nature.

In this work, we present our optical polarimetric measurements and time-resolved spectral data in the region of Hα for RX J1141.3-6410. Some modeling of the intensity and polarization has been made. We suggest a possible geometrical configuration for RX J1141.3-6410 and the main regions of line formation based on the polarization models and the spectroscopic data.

Send offprint requests to: C. V. Rodrigues, (claudia@das.inpe.br)

⋆ This work was based on observations made at Laboratório Nacional de Astrofísica/CNPq/MCT, Brazil.

2. Observations and data reduction

2.1. Polarimetric acquisition and reduction

The polarimetric observations were made during two nights (March 04-05, 1997) with the 1.60 m telescope of the *Laboratório Nacional de Astrofísica* (LNA), Brazil. We used a CCD camera modified by a polarimetric modulus (Magalhães et al. 1996). All measurements were made using a R_C filter.

The polarimetric modulus consists of a fixed analyzer (calcite prism), a $\lambda/4$ retarder waveplate and a filter wheel. The retarder plate is rotated with $22\overset{\circ}{.}5$ steps. Therefore, a polarization measurement consists of (a minimum of) eight integrations in subsequent retarder orientations. The calcite block separates the extraordinary and ordinary beams by $12''$. This division eliminates any sky polarization (Piirola 1973; Magalhães et al. 1996). The $\lambda/4$ retarder allows us to measure the circular and linear polarization simultaneously.

Our main goal was to measure the circular polarization (V) with an error of the order of 1% and a time resolution enough to check a variability locked with the photometric modulation. Therefore, we chose a time integration of 90 s for each individual image. In this way, a V point spans 8×90 s (720 s) plus the dead time. We would usually group the images in sequences of 8 images with no overlap (images 1 through 8, images 9 through 16 and so on). However, in order to improve the temporal resolution we have grouped the images with overlap (images 1 through 8, images 2 through 9 and so on). In this way, we have a time interval between two points of typically 140 s (90 s + dead time). These data also enable us to perform differential photometry using comparison stars in the field.

The basic reduction of the polarimetric data is identical to the photometric one. This step was performed using standard IRAF[1] routines for image correction and photometric analysis. The derived counts were the input for a FORTRAN code that calculates the polarization (Magalhães et al. 1996; Magalhães et al. 1984). However, in those works, one cannot find the solution for the Stokes parameters using a $\lambda/4$ plate, which is presented below.

The intensities of the two images in the CCD, ordinary (I_o) and extraordinary (I_e) ones, are related to the Stokes parameters (I, q, u, v) of the incident beam by (Serkowski 1974):

$$2I_{o,e} = I \pm q\cos^2 2\theta \pm u \sin 2\theta \cos 2\theta \mp v \sin 2\theta,$$

where θ is the waveplate position angle. The upper and lower signals refer to each of the two images.

The normalized Stokes parameters (Q=q/I, U=u/I and V=v/I) can be obtained using the method of Magalhães et al. (1984) applied to a $\lambda/4$ retarder. Defining the quantity z_i for each retarder position, i:

$$z_i = \frac{I_{e,i} - I_{o,i}}{I_{e,i} + I_{o,i}},$$

we obtain the following expressions for the Stokes parameters (assuming eight retarder positions):

$$\begin{aligned} Q &= \frac{1}{3}\sum z_i \cos^2 2\theta_i, \\ U &= \sum z_i \sin 2\theta_i \cos 2\theta_i, \\ V &= -\frac{1}{4}\sum z_i \sin 2\theta_i, \end{aligned}$$

where θ_i is the retarder position angle.

The first position of the retarder did not correspond to zero degree. But, it was possible to determine its alignment by minimizing the errors in V. We are confident that this procedure gives us a good estimate of the zero point by the results obtained for the observed standard stars. However, we could not solve an indetermination of 180°. Because of that we could only measure the V modulus, not its signal.

One of the images of RX J1141.3-6410 was contaminated by the superposition of a much fainter neighbour star. We did the photometry of the other image of the superposed star, which was isolated, and these counts were subtracted from those of RX J1141.3-6410. We have performed the reduction using different combinations of apertures for RX J1141.3-6410 and the superposed star and also using no correction at all. The circular polarization was practically not affected by this procedure. On the other hand, the linear polarization was sensitive to the parameters used in the correction. Therefore, the linear polarization results must be taken with care.

The results of circular polarimetry and differential photometry are presented in Fig. 1. The average error in V is 0.82%. The errorbars of the linear polarization prevent us to detect any polarization less than 4%. Within this limit, no linear polarization was detected in any orbital phase.

2.2. Orbital ephemeris

The light curve shown in the previous section can be used to refine the orbital ephemeris of Cieslinski & Steiner (1997). Additional R_C photometry were obtained on 1997 April 15-16-19 with the Boller & Chivens 60 cm telescope at LNA, using a CCD camera. The new ephemeris for the maximum photometric optical flux is:

$$T_{max}(HJD) = 2\,450\,356.46655(\pm 3) + 0.131\,517\,8(\pm 3)E.$$

All orbital phases quoted in this paper refer to the above ephemeris.

2.3. Spectroscopic data

We obtained 30 spectra with 10 minutes of integration time on April 14, 1997 with the 1.60 m telescope of the LNA. We used the Cassegrain spectrograph with a 1200 line mm^{-1} grating and a CCD detector. This configuration gave a spectral resolution of about 2 Å and a covered wavelength region between 6100 and

[1] IRAF is distributed by National Optical Astronomy Observatories, which is operated by the Association of Universities for Research in Astronomy, Inc., under contract with the National Science Foundation.

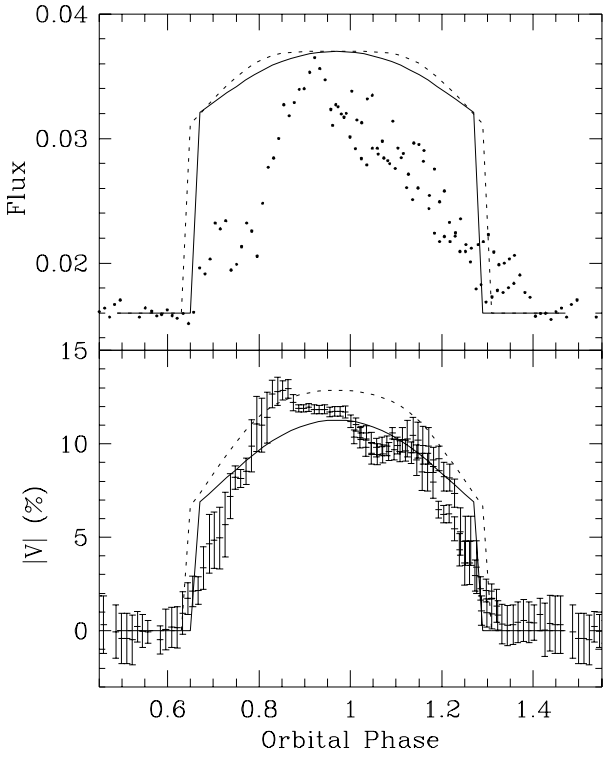

Fig. 1. Differential photometry and circular polarization of RX J1141.3-6410. The abscissa corresponds to the orbital phase using the new ephemeris of Sect. 2.2. The lines represent the model of Wickramasinghe & Meggitt (1985) with an electronic temperature of 10 keV and Λ equals to 10^5 (see Sect. 3.1). The full line corresponds to a model with: $i = 5°$, $\beta = 87°$. The dotted line corresponds to a model with: $i = 85°$, $\beta = 8°$. Both models have a magnetic field strength of 30MG

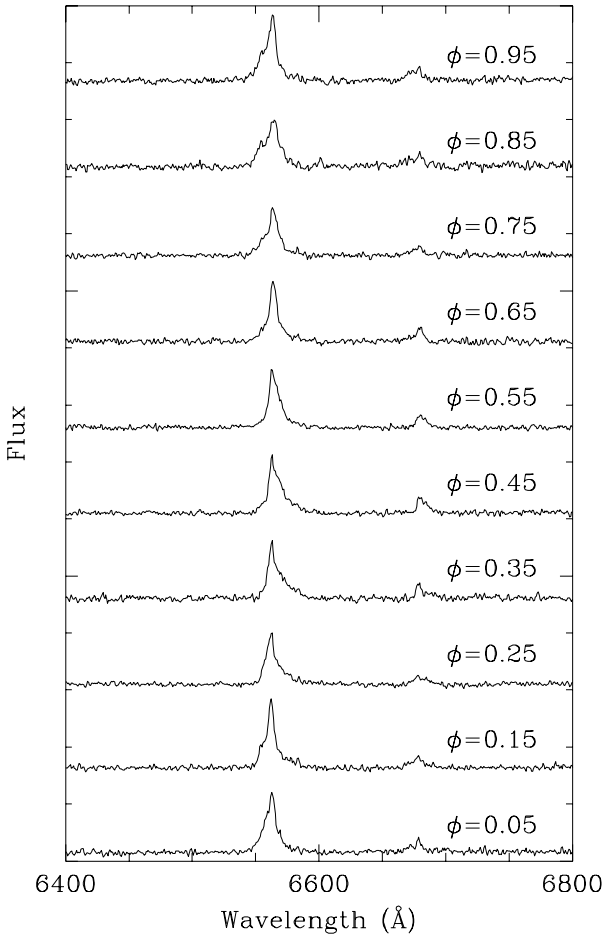

Fig. 2. Spectra of RX J1141.3-6410 binned in 10 orbital phases

6970 Å. We used a 200μm slit which corresponds to 2″ in the sky. This was approximately the seeing in that night. A GG385 order blocking filter was also used. The reduction was made using the standard routines of the IRAF package. The spectra were flux calibrated using the spectrophotometric standard stars from Stone & Baldwin (1983) and Taylor (1984). Fig. 2 shows the spectra binned in 10 orbital phases (see discussion below). The Hα and He I λ6678 lines are present.

Albeit the small range in wavelength, we have searched for some indicative of a cyclotron component in the spectra. For this we have averaged the spectra corresponding to the faint and bright photometric phases separately. Within the wavelength range and the signal to noise ratio of our spectra, no difference in the continua could be noted.

In order to check the existence of periodicity in the spectroscopic data, we have calculated the radial velocity of both lines using the Double Gaussian method described by Schneider & Young (1980) and Shafter (1985). This method measures the radial velocity of the line wings. Therefore, it provides us with the radial velocity of the broad base component. The Double Gaussian method requires two adjustable parameters: the Gaussian width, σ, and the distance between the curves, $2a$. They have been chosen by the minimization of the σ_K/K, where K is the semi-amplitude of the radial velocity curve. The K-amplitude has been obtained from the fit of a sinusoidal model. For the Hα line, we have found: σ = 12 Å and a = 8 Å. The Discrete Fourier Transform method applied to the derived radial velocities has given a spectroscopic period of 0.1290 $\pm$ 0.0022 d. This value is completely consistent with the photometric one within one sigma uncertainty. The result for the He I λ6678 line is also consistent with the photometric period, but the errorbar is higher. Based on the agreement between the photometric and spectroscopic periods, we have combined the original data in ten spectra according to the photometric orbital phase (see Fig. 2).

An inspection of the spectra shows that the emission lines may be formed by more than one component, which is common in this type of star. So we have deconvolved the Hα line using two Gaussian functions. The He I λ6678 line was too noisy preventing this analysis (see Fig. 2). The two Gaussian fit of the spectral profile has been done using the *splot* routine of IRAF. In order to constrain the parameters to be adjusted, we have again applied the Double Gaussian method to the combined spectra and the obtained central wavelengths of the broad component have been assumed fixed. The best fit has been found for: σ = 10 Å and a = 19 Å. The increase in the separation of the

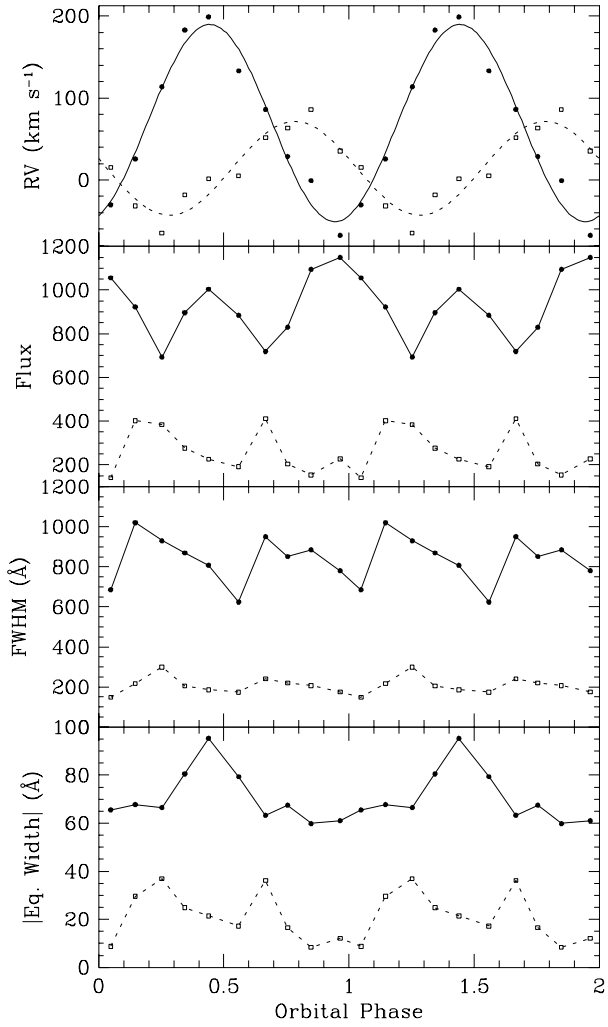

Fig. 3. Radial velocities, flux, FWHM and equivalent widths of the broad and narrow components of the Hα line of RX J1141.3-6410 obtained using a two Gaussian fit. The curves in the radial velocity panel correspond to the fitted sinusoidal model (see Table 1)

two Gaussian for the combined spectra reflects the higher signal/noise which has allowed us to detect the line further from the peak.

The results for the radial velocities, flux, FWHM and equivalent width are shown in Fig. 3. The widths (FWHM) have not been deconvolved from the instrumental resolution which is around 90 km s^{-1}. Assuming the radial velocity of the broad component as a free parameter, the flux, equivalent width and FWHM do not practically change. However, the departure of the radial velocity relative to a sinusoidal curve increases: the maximum redshift tends to occur at smaller phases (≈0.35) and the maximum blueshift remains at the same location. The radial velocity curves of Fig. 3 have been fitted using a standard sinusoidal model, whose results are shown in Table 1 and Fig. 3. Using the individual 30 spectra, we have obtained similar values for the broad component. For instance, the K-amplitude is K=110.5 ± 5.8.

Table 1. Radial velocities parameters of the broad and narrow components of the Hα line of RX J1141.3-6410

Parameter	Broad Comp.	Narrow Comp.
K (km s^{-1})	120.2 ± 8.2	57.1 ± 7.8
γ (km s^{-1})	69.5 ± 5.9	14.2 ± 5.5
$\phi_o^{\rm a}$	0.444 ± 0.011	0.783 ± 0.022

[a] This phase corresponds to the maximum redshift of the component

3. Discussion

3.1. What the polarization of RX J1141.3-6410 can tell us

Fig. 1 shows the flux (in arbitrary units) and the circular polarization (modulus) of RX J1141.3-6410. A high degree of circular polarization is present in a large fraction of its period with a maximum value of approximately 13%. This confirms the classification of RX J1141.3-6410 as a polar. This figure also shows a clear correlation between flux and polarization. The phases of null polarization coincide with the photometric minimum indicating that in these phases the accretion region is out of the line of sight. Whatever the signal of V is, no change in the signal is observed (because V crosses the zero axis once). This indicates that in this wavelength region we probably see only one pole or regions of same polarity.

We have fitted our results on flux and circular polarization using the models of Wickramasinghe & Meggitt (1985, hereafter WM85) for a point-like accretion region. This region must be extended (Mukai 1988), but a point-like model can provide us with some insight into the geometrical and physical configuration of RX J1141.3-6410. In order to do the fits, we have assumed two components: (1) a component which is constant along the orbital period and whose polarization is null; and (2) a component coming from the accretion region whose intensity and polarization are assumed to be represented by the WM85 models. We have normalized the WM85 intensity values to fit the maximum value of the second component. With the above assumptions, the circular polarization, V, can be also determined without any extra normalization. So the level and the shape of the circular polarization can be fitted.

The phase duration of constant flux and polarization (V = 0%) can be identified with the phase where the accretion region is occulted from the observer. This phase interval, $\Delta\phi$, depends only on the geometry of the system and defines a relation between the orbital inclination, i, and the colatitude of the magnetic field, β (Bailey & Axon 1981):

$$\cos \pi\Delta\phi = \frac{1}{\tan i \tan \beta}. \quad (1)$$

From Fig. 1, we see that this phase interval is around 0.30. So hereafter we will define the geometry only by the inclination, since the above relation fixes the value of β.

We could find reasonable fits to all combinations of electron temperature and size parameter, Λ, presented by WM85. Examples are shown in Fig. 1. It should be noted, however, that V is

better adjusted than the flux (see Fig. 1). This is consistent with the results of Piirola et al. (1990) who used the calculations of WM85 to construct a model for an extended emitting region. Their results show that the flux is more modified than the circular polarization relative to the point-like model (see their Fig. 5). For an extended region the flux tends to have a smaller flat top and consequently a larger phase interval of increasing (and decreasing) flux. Therefore the changes caused by the extension of the emitting region and possible gradients in the physical conditions would improve the agreement between the model and our data.

Considering only the curve shapes, we could get a hint about the orbital inclination of RX J1141.3-6410 (and consequently β). The model indicates two possible solutions: small inclinations (around 5°) or large inclinations ($\approx 85°$). For intermediate values, the polarization and flux curves present peaks or are not correlated. This happens because the intensity and polarization have opposite behaviours as α varies, where α is the angle between the line of sight and the dipole axis of the magnetic field (WM85). This implies that a correlation between intensity and polarization could only be achieved if α does not change so much. As we have a phase where α must be around 90° (the phase when there is a transition from a visible to a hidden column), α must be restricted around this value. Using Eq. 1, the colatitude of the magnetic field axis is about 0° for inclinations near 90°. If the system is seen face on, β must be near 90°. The numerical solutions for the intensity and circular polarization are exactly the same if one considers $(\pi - i)$ and $(\pi - \beta)$.

Assuming a fixed geometry and one of the WM85 models, the polarization modulus depends basically on the magnetic field strength. We have found values restricted to the range between 15 and 40 MG.

There is no evidence of eclipses in the light curve of RX J1141.3-6410. This can impose a limit to its inclination angle. First, let's estimate the maximum inclination, i_{max}, that allows a non-eclipsing system. It can be seen that:

$$\sin(\frac{\pi}{2} - i_{max}) = \frac{R_2}{a}, \quad (2)$$

where R_2 is the secondary radius and a is the distance between the stars. The secondary radius can be approximated by the size of its Roche lobe. So, one could use the expressions of Paczynski (1971) for R_2/a in order to obtain i_{max}. These relations depend on the mass ratio of the system, q.

Using the relation of Patterson (1984) between the mass of the secondary, M_2, and the orbital period in cataclysmic variables, we obtain $M_2 = 0.28M_\odot$. The average primary mass of a magnetic cataclysmic variable is $0.79 \pm 0.11M_\odot$ (Webbink 1990). This gives us an approximate value to q of 0.36. This corresponds to i_{max} equal to 73°. Assuming values of the primary between 0.6 and $1.4M_\odot$, the i_{max} range is 71.°6 to 75.°3. The WM85 models with an inclination of 75° produce a circular polarization quite different from the observed (much more peaked). So the models of the cyclotron component tend to favour very low values for the inclination.

3.2. Emission lines in RX J1141.3-6410

Like the polarization and optical flux, the orbital variation of the emission line components depends on the geometrical and physical configuration of RX J1141.3-6410. Below, we present some discussion on the spectroscopic data presented in Sect. 2.3.

The narrow component of polars can be associated with the irradiated surface of the secondary or the stream. In RX J1141.3-6410, we favour the interpretation that the narrow component is due to the horizontal stream. The main argument is the relatively high (deconvolved) width of this component which can reach more than 200 km s^{-1} (Mukai 1988). The orbital dependence of the flux can also give us some information about the region of line formation. The flux of a component originated on the secondary surface has only one peak during the orbital period (e.g., Schwope et al. 1997; Beuermann & Thomas 1990). It occurs at the superior conjunction of the secondary when the largest fraction of its irradiated surface is exposed to the observer. On the other hand, an optically thick stream has its maximum flux when it is seen sideways (Mukai 1988). This produces two peaks during one orbital period. The flux of the narrow component is not very accurately determined, but there is a small evidence for two peaks along the period. So that could also indicate that the stream is the main contributor to the narrow component. The K-amplitude of the narrow component radial velocity is small ($\approx$ 60 km s^{-1}). Any movement in the orbital plane would have small radial velocities, if the system is seen near pole on - as the absence of eclipses seems to indicate. Therefore the K-amplitude could not help in disantagling the origin of the narrow component.

The understanding of the geometrical configuration of RX J1141.3-6410 would be improved if we had some information about the secondary phasing. This could be directly obtained through eclipses, absorption lines or ellipsoidal variations. Unfortunately, none of them is available for this star. The blue-to-red phasing of the radial velocities of lines formed in the horizontal stream usually presents a small offset relative to the inferior conjunction of the secondary between -0.05 and -0.3 (Mukai 1988). If the narrow component is indeed produced in the horizontal stream, the inferior conjunction of the secondary would occur near phase 0.6. This puts the accretion region on the WD face opposite to the secondary. Most polars seem to have the active pole facing the secondary (Cropper 1990), contrary to what is seen is RX J1141.3-6410, if the above suppositions are correct.

About the narrow component, we could also say that if it is produced in the orbital plane of the system, which is valid for the stream or the secondary surface, the gamma velocity, γ, can be associated with the systemic velocity of the binary.

The K-amplitude of the broad component in polars can reach 1000 km s^{-1} (Warner 1995). This makes the values found for RX J1141.3-6410 relatively small ($\approx$120 km s^{-1}). This result is consistent with the polarization models, since they imply that we are seeing the column edge on (α is approximately 90°). So the material falling down to the white dwarf has its larger velocity component perpendicular to the line of sight.

The broad component flux does not seem to be occulted (as the cyclotron component is), this can be an indication that it is formed at higher distances from the white dwarf than the cyclotron component. This supposition is consistent with the behaviour of its the equivalent width. It has one maximum in the phase interval where the (polarized) cyclotron component is occulted by the white dwarf. The flux of the broad component has two maxima in one period. They occur near the maximum red and blueshift. In the maximum redshift phase (minimum photometric flux) there seems to be a slightly smaller flux than in the blueshift peak.

The width of the broad component presents two peaks during the orbital period. It is consistent with the model by Ferrario et al. (1989) of the radial velocity and width of the broad component. For some models, the width has two peaks which are not necessarily coincident with the maximum projected velocities (see their Fig. 6). More than that, the difference between maximum radial velocity and maximum width increases with the distance of the emission forming region from the WD.

The broad component of RX J1141.3-6410 has its maximum redshift approximately half a period after the maximum polarization. This is not usual for polars, which commonly present the maximum redshift at the same phase of the maximum circular polarization (Liebert & Stockman 1985). The last happens when the accretion column is aligned with the line of sight. Because of that, Liebert & Stockman associated the broad component with the accretion funnel. However, Doppler tomography of polars (Diaz & Steiner 1994; Schwope et al. 1997; Šimić et al. 1998) shows that the bulk of the broad component seems to be produced near the coupling region. We suggest that the broad component could possibly come from the coupling region. As the polarization must come from a region nearer the WD (the falling region), this configuration could explain the blueshift in the broad component at the same phase of maximum circular polarization. However, we probably see only a small component of the velocity, so these conclusions must be taken with care.

If the broad component is indeed formed in the coupling region of RX J1141.3-6410, it is equivalent to say that it is formed in the rising part of the accretion stream. This means that V_z of this component is positive. In order to get a γ velocity positive the inclination of the system must be greater than 90°. For RX J1141.3-6410, particularly, this means around 180°.

4. Conclusion

The high level of circular polarization observed in RX J1141.3-6410 confirms this star as a polar. Within our data precision, no peak in linear polarization was observed. The Hα line of RX J1141.3-6410 shows two components. The maximum blueshift of the broader component is locked with the maximum circular polarization, contrary to most polars.

We suggest that the system is seen near face on and that the magnetic field axis lies near the orbital plane. This configuration is able to explain the main features of RX J1141.3-6410 data. The narrow component seems to be produced in the horizontal stream, while the broad component may have its origin in the coupling region.

Acknowledgements. We are very thankful to the referee's suggestions which helped to improve the paper. We acknowledge Dr. M. P. Diaz by his careful reading of the manuscript. We are grateful to M. G. Pereira for sharing telescope time. CVR and DC would also like to acknowledge Dr. F. J. Jablonski for the discussions and his help with photometric analysis. Finally, we are also thankful to A. Pereyra and A. M. Magalhães for providing their IRAF routines which facilitate the polarimetric reduction.

References

Bailey J., Axon D. J., 1981, MNRAS 194, 187
Beuermann K., Thomas H. C., 1990, A&A 230, 326
Cieslinski D., Steiner J. E, 1997, MNRAS 291, 321
Cropper M., 1990, Space Sci. Rev. 54, 195
Diaz M. .P., Steiner J. E., 1994, A&A 283, 508
Ferrario L., Wickramasinghe D. T., Tuohy I. R., 1989, ApJ 338, 832
Liebert J., Stockman H. S., 1985, in: D. Q. Lamb, J. Patterson (eds.) Cataclysmic Variables and Low Mass X-Ray Binaries, D. Reidel Publ. Co., Dordrecht, p. 151
Magalhães A. M., Benedetti E., Roland E., 1984, PASP 96, 383
Magalhães A. M., Rodrigues C. V., Margoniner V. E., Pereyra A., Heathcote S., 1996, High Precision CCD Imaging Polarimetry. In: Roberge W. G., Whittet D. C. B. (eds.) Polarimetry of the Interstellar Medium. Astronomical Society of Pacific, San Francisco, p. 118
Motch C., Haberl F., Guillout P., et al., 1996, A&A 307, 459
Mukai K., 1988, MNRAS 232, 175
Paczynski B., 1971, ARAA 9, 183
Patterson J., 1984, ApJ Suppl. 54, 443
Piirola V., 1973, A&A 27, 383
Piirola V., Coyne G. V. and Reiz A., 1990, A&A 235, 245
Rosen S. R., Mason K. O., Cordova F. A. 1987, MNRAS 224, 987
Schneider D. P., Young P., 1980, ApJ 238, 946
Schwope A. D., Mantel K.-H., Horne K., 1997, A&A 319, 894
Serkowski K., 1974, Polarimeters for Optical Astronomy. In: Gehrels T. (eds.) Planets, Stars, and Nebulae Studied with Photopolarimetry. Univ. Arizona Press, Arizona, p. 135
Shafter A. W., 1985, In: Lamb D. Q., Patterson J. (eds.) Cataclysmic Variables and Low Mass X-Ray Binaries, D. Reidel Publ. Co., Dordrecht, p. 355
Šimić D., Barwig H., Bobinger A., Mantel K.-H., Wolf S., 1998, A&A 329, 115
Stone R. P. S., Baldwin J.A., 1983, MNRAS 204, 347
Taylor B. J., 1984, ApJS 54, 259
Warner B., 1995, Cataclysmic Variable Stars. Cambridge Univ. Press, Cambridge
Webbink R. F., 1990, Absolute parameters of Cataclysmic Variables. In: Mauche C. W. (eds) Accretion-powered compact binaries, Cambridge Univ. Press, Cambridge, p. 39
Wickramasinghe D. T., Meggitt S. M. A., 1985, MNRAS 214, 605 (WM85)